Cell Death and Differentiation (2012) 19, 1983–1991

www.nature.com/cdd

Unveiling an exceptional zymogen: the single-chain form of tPA is a selective activator of NMDA receptor-dependent signaling and neurotoxicity

J Parcq[1], T Bertrand[1], A Montagne[1], AF Baron[1], R Macrez[1], JM Billard[2], A Briens[1], Y Hommet[1], J Wu[3], M Yepes[3], HR Lijnen[4], P Dutar[2], E Anglés-Cano[1,5] and D Vivien*[,1,5]

Unlike other serine proteases that are zymogens, the single-chain form of tissue plasminogen activator (sc-tPA) exhibits an intrinsic activity similar to that of its cleaved two-chain form (tc-tPA), especially in the presence of fibrin. In the central nervous system tPA controls brain functions and dysfunctions through its proteolytic activity. We demonstrated here, both *in vitro* and *in vivo*, that the intrinsic activity of sc-tPA selectively modulates *N*-methyl-D-aspartate receptor (NMDAR) signaling as compared with tc-tPA. Thus, sc-tPA enhances NMDAR-mediated calcium influx, Erk(½) activation and neurotoxicity in cultured cortical neurons, excitotoxicity in the striatum and NMDAR-dependent long-term potentiation in the hippocampal CA-1 network. As the first demonstration of a differential function for sc-tPA and tc-tPA, this finding opens a new area of investigations on tPA functions in the absence of its allosteric regulator, fibrin.
Cell Death and Differentiation (2012) **19,** 1983–1991; doi:10.1038/cdd.2012.86; published online 29 June 2012

Serine proteases display critical functions in inflammation, blood clotting and fibrinolysis. Activation of their inactive precursors by limited proteolysis regulates their activity. Thus, plasminogen and prothrombin must be cleaved into their two-chain form to display full enzymatic activity. In the vascular compartment, tissue plasminogen activator (tPA) mainly secreted by endothelial cells[1] promotes fibrinolysis via the conversion of fibrin-bound plasminogen into plasmin. Although, the secreted single-chain tPA (sc-tPA) can be processed into its two-chain form (tc-tPA) by plasmin or kallikrein,[2,3] sc-tPA is an unusually active zymogen (high intrinsic proteolytic activity, low zymogenicity) that does not require proteolytic processing to be active but the presence of its allosteric regulator, fibrin. In the vasculature, it is well established that fibrin stimulates the enzymatic activity of sc-tPA and tc-tPA to similar levels.[2,4] tPA has also critical functions in the brain parenchyma either as an enzyme, a cytokine-like molecule or a neuromodulator with roles in cell migration, neuronal plasticity and neurodegeneration.[5–7] Neurons[8] and glial cells[9,10] secrete tPA in the brain parenchyma where it can controls some plasminogen-dependent effects. For instance, it was proposed that the tPA-mediated generation of plasmin controls the degradation of the extracellular matrix to promote neuronal death.[11–13] There are also evidences that tPA mediates a number of plasminogen-independent functions on non-fibrin substrates. These substrates, binding proteins or receptors for tPA include the platelet-derived growth factor-C,[14] the low density lipoprotein receptor-related protein,[10] annexin-II,[9,15] the chemokine macrophage chemoattractant protein, macrophage chemoattractant protein-1[16] and the *N*-methyl-D-aspartate receptor (NMDAR).[6] It is now well established that the interaction of tPA with the NMDAR leads to an increased calcium influx, activation of Erk(½) and neuronal death.[7] Thus, tPA influences plasminogen-dependent and -independent mechanisms with up to now no major differential functions reported between sc-tPA and tc-tPA. Here we report that in the brain parenchyma the intrinsic proteolytic activity of sc-tPA is involved in NMDAR-dependent signaling in cortical neurons (Erk(½) activation, neurotoxicity), in the striatum (excitotoxicity) and in the hippocampal CA-1 network (long-term potentiation (LTP) facilitation). This is the first demonstration of a function for the non-zymogen sc-tPA compared with tc-tPA (Figure 1).

Results

To investigate whether sc- and tc-tPA have similar effects on the NMDAR, we have used different sources of human tPA: human recombinant tPA (Actilyse, rtPA, 90–95% sc-tPA),

[1]Inserm U919, Serine Proteases and Pathophysiology of the neurovascular Unit, Université de Caen Basse-Normandie, GIP Cyceron, Caen, France; [2]Inserm U894, Centre de psychiatrie et de Neurosciences, Université Paris Descartes, Paris, France; [3]Department of Neurology, Center for Neurodegenerative Disease, Emory University School of Medicine, Atlanta, GA, USA and [4]Center for Molecular and Vascular Biology, KU Leuven, Leuven, Belgium
*Corresponding author: D Vivien, Inserm U919, Serine Proteases and Pathophysiology of the neurovascular Unit, Université de Caen Basse-Normandie, 14 Boulevard Henri Becquerel, GIP Cyceron, Caen 14000, France. Tel: +33 2 31 47 01 66; Fax: +33 2 31 47 02 22; E-mail: vivien@cyceron.fr
[5]These authors contributed equally to this work.
Keywords: tissue plasminogen activator; protease; zymogen; neurotoxicity; long-term potentiation
Abbreviations: tPA, tissue plasminogen activator; CNS, central nervous system; NMDA, *N*-methyl-D-aspartate; LTP, long-term potentiation; LTD, long-term depression; EACA, 6-aminocaproic acid; D-APV, D-2-amino-5-phosphonovalerate; PAI, plasminogen activator inhibitor; NS, neuroserpin
Received 19.10.11; revised 25.5.12; accepted 28.5.12; Edited by L Greene; published online 29.6.12

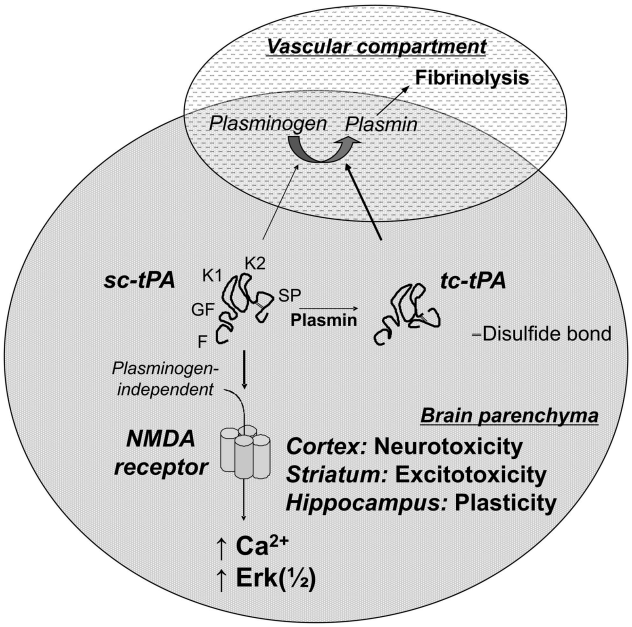

Figure 1 tPA is a mosaic protein consisting of five distinct modules: a finger domain (F), an epidermal growth factor-like domain (EGF), two kringle domains (K1 and K2) and a serine protease proteolytic domain (SP). Secreted sc-tPA can be converted to its two-chain (tc-tPA) form by plasmin. Both sc-tPA and tc-tPA display an equivalent efficacy for plasmin-induced fibrinolysis in the vascular compartment. In contrast, sc-tPA is the primary effector of plasminogen-independent but proteolytically mediated NMDA-induced neurotoxicity, calcium influx and NMDA-dependent Erk(½) activation on cortical neurons. Similarly, sc-tPA modulates NMDA receptor-induced neuronal plasticity by enhancing long-term potentiation on hippocampal slices

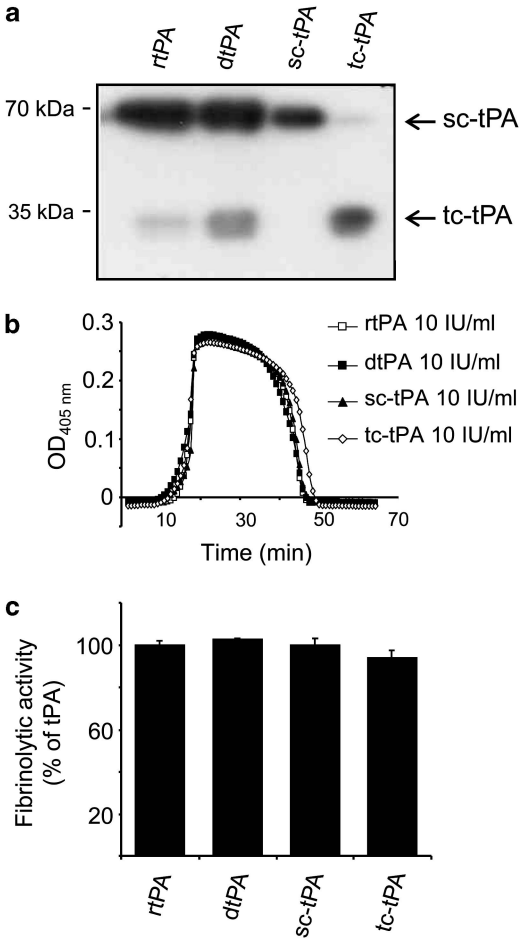

Figure 2 sc-tPA and tc-tPA display an equivalent fibrinolytic activity. (**a**) SDS-PAGE followed by immunoblotting of rtPA, dtPA, sc-tPA and tc-tPA (200 ng per lane). (**b** and **c**) Fibrinolytic activity of the different forms of tPA normalized to an International Reference (IRP 98/714) using the half-time for clot lysis

a dialyzed tPA prepared from rtPA (dtPA, 90–95% sc-tPA), a mAb-purified human sc-tPA (sc-tPA, 100% sc-tPA) and a human tc-tPA purified following treatment of rtPA with plasmin (tc-tPA, 100% tc-tPA) (Supplementary Table 1). Each preparation was characterized by immunoblotting (Figure 2a) and its ability to initiate fibrinolysis. In agreement with previous reports,[2,4] rtPA, dtPA, sc-tPA and tc-tPA displayed similar fibrinolytic activity as revealed by *in vitro* clot lysis (Figures 2b and c). However, as cleavage of the NMDA receptor GluN1 subunit by tPA does not require fibrin, the different sources of tPA were tested by reference to their fibrin-independent amidolytic activity against a fluorogenic substrate (Spectrofluor 444FL), and confirmed by using plasminogen-casein zymography (Figures 3a–d), unless otherwise stated.

Enhanced NMDA-dependent excitotoxicity was tested on primary cultures of cortical neurons, 24 h after an 1 h exposure with 50 μM NMDA either alone or in the presence of the different sources of tPA cited above. As expected, NMDA-induced excitotoxicity was potentiated in the presence of rtPA ($n=4$, $P<0.01$) or dtPA ($n=4$, $P<0.01$) excluding buffer bias (particularly, the putative presence of low molecular weight contaminants[17] or the high concentration of arginine present in the commercial preparation,[18] Figure 4a). Although rtPA and the mAb-purified sc-tPA promoted NMDA-mediated excitotoxicity by around 50% (75% and 77% neuronal death respectively *versus* 51% in the presence of NMDA alone; $n=4$, $P<0.01$), tc-tPA failed (Figure 4b). The slight basal neurotoxicity exhibited by sc-tPA (less than 20%) may be due to the presence of endogenous glutamate (Figure 4b). Site-inactivated dtPA (dGGACK-tPA) (Figure 4c) also failed to promote NMDA-induced neurotoxicity (Figure 4d) ($P<0.01$, $n=3$). Thus, on primary cultures of cortical neurons only the proteolytically active form of sc-tPA promotes NMDAR-dependent excitotoxicity. Parallel experiments were performed *in vivo*, in a model of NMDA-induced excitotoxic injury in mice with intrastriatal coinjection of NMDA and either sc-tPA or tc-tPA (Figure 4e). As observed *in vitro*, 24 h after tPA injection, only the sc-tPA promoted NMDA-dependent excitotoxic brain damage as evaluated by thionine staining (with excitotoxic lesions of 8.00 mm^3 ± 0.99 for NMDA alone *versus* 12.85 mm^3 ± 1.67 for NMDA supplemented with sc-tPA, $n=4$, $P<0.05$).

To determine whether differential effects of sc-tPA and tc-tPA on neurotoxicity are selective or just a threshold effect, a range of increasing concentrations of both forms of tPA were tested regarding their respective ability to promote NMDAR-mediated neurotoxicity (Figure 5). Although sc-tPA promoted NMDA receptor- mediated neurotoxicity in a dose-dependent manner from 60 to 300 nM with an IC_{50} of around 100 nM,

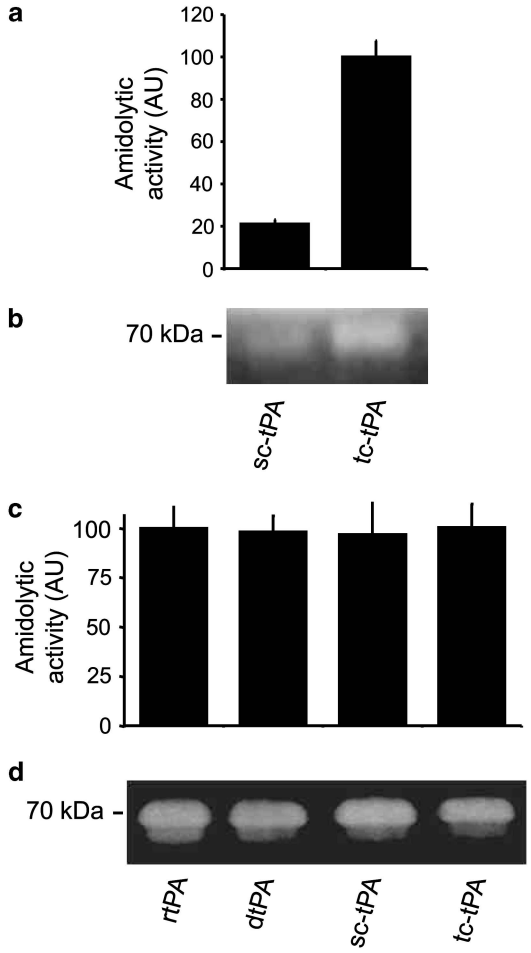

Figure 3 In the absence of fibrin, tc-tPA displays an enzymatic activity higher than sc-tPA. (**a** and **b**) Activity of sc-tPA and tc-tPA (60 nM) measured either on a fluorogenic substrate (**a**) or by plasminogen-casein zymography assay (**b**). Similar amidolytic activity of sc-tPA and tc-tPA was observed in the presence of a five times higher concentration of sc-tPA as measured with a fluorogenic substrate (**c**) or by plasminogen-casein zymography assay (**d**). Activities of rtPA, dtPA, sc-tPA and tc-tPA were normalized to amidolytic activity (**c** and **d**) and corresponding concentrations used for the next experiments

tc-tPA failed to potentiate NMDA-mediated neurotoxicity at any of the concentrations tested (Figures 5a and b). This observation is independent of their respective proteolytic activity, as sc- and tc-tPA displayed similar dose-dependent fibrinolytic activity (Supplementary Figures 1a and b), and as previously reported.[3,4] In addition, cultures of cortical neurons were subjected to NMDA paradigm as described above in the presence of 60 nM tPA (final total molar concentration) at different sc-tPA to tc-tPA ratios (40 : 60; 60 : 40; 80 : 20; 100 : 0) (Figure 5c, $n=4$). Altogether, these data show that the NMDA neurotoxicity of tPA is sc-tPA dose-dependent regardless of the presence of tc-tPA.

As tPA-mediated plasmin formation was also reported to control NMDAR-dependent signaling,[19] we tested whether plasmin could influence tPA-mediated NMDA neurotoxicity *in vitro*. Exogenous plasmin alone (100 nM) did not influence NMDA-mediated neurotoxicity. However, treatment of neurons with exogenous plasmin prevented the NMDA neurotoxicity of sc-tPA (Figure 6a) ($n=4$, $P<0.01$) by promoting the conversion of sc-tPA into tc-tPA (representative immunoblot; Figure 6a, insert). In neuronal cultures maintained in the presence of either 6-aminocaproïc acid (EACA, 25 mM) or aprotinin (1 μM) to prevent endogenous plasmin formation in the incubation medium or on the cell monolayer[20] (Supplementary Figure 2), sc-tPA remained neurotoxic in the presence of NMDA (Figures 6b and c), further supporting the hypothesis that sc-tPA promotes NMDAR functions through a plasminogen-independent mechanism. In agreement with our *in vitro* data, α2-antiplasmin (500 nM) did not abolish sc-tPA-induced potentiation of NMDA-induced excitotoxicity when injected into the striatum of swiss mice (Figures 6d and e, $9.24\,mm^3 \pm 0.98$ for NMDA and $12.34\,mm^3 \pm 2.36$ for NMDA + sc-tPA in the presence of α2-antiplasmin, $n=7$, $P<0.05$, compared with $8.90\,mm^3 \pm 2.13$ for NMDA alone and $13.08\,mm^3 \pm 1.95$ for NMDA + sc-tPA in control conditions, $n=7$, $P<0.01$). To address the concern of the endogenous plasmin inhibition, zymography assay were performed (20 μg of protein extracts) from perfused striata of swiss mice receiving intrastriatal injection of NMDA alone (10 mM) or with a combination of sc-tPA (45 μM) and α2-antiplasmin (100 nM). No active plasmin was observed in the different conditions tested (Figure 6e, representative of $n=4$ animals per group). Similarly, when tested on plasminogen-deficient mice, sc-tPA was still capable to promote NMDA-induced excitotoxic lesions ($31.8\,mm^3$ for NMDA alone *versus* $37.4\,mm^3$ for NMDA + sc-tPA, $n=5$, $P<0.05$, Figure 6f). Altogether, these *in vivo* data confirm that sc-tPA promotes NMDAR signaling through a plasminogen-independent mechanism.

As NMDA-induced calcium influx is one of the early events triggered in NMDA-mediated signaling,[21] we tested the ability of the different forms of tPA to influence this parameter in cortical neurons (Figures 7a–c). Although dtPA (not shown) and sc-tPA potentiated NMDA-induced calcium influx (+ 34% compared with NMDA stimulation, Figures 7a and c), tc-tPA did not (Figures 7b and c) (three independent experiments, $n>120$ cells, $P<0.05$). These data provide additional evidence for a differential effect of sc-tPA and tc-tPA on NMDAR-dependent signaling. tPA was also reported to promote NMDAR-induced Erk(½) activation, an effect directly linked to its neurotoxicity.[22] Here again, whereas sc-tPA induced an increase in NMDA-mediated Erk(½) activation (+ 19%, $n=3$, $P<0.05$), an equimolar concentration of tc-tPA did not (0.3 μM, Figure 7d), but rather induced a significant decrease (− 50.5%, $n=3$, $P<0.05$). Thus, at the doses used, only sc-tPA promotes NMDA-induced neurotoxicity and Erk(½) activation. This is the first evidence of a differential effect of sc-tPA and tc-tPA on NMDAR signaling-mediated neurotoxicity.

tPA was also reported to modulate the magnitude of LTP,[23] an effect mediated through NMDAR.[5] We observed that although sc-tPA potentiated the hippocampal NMDAR-dependent LTP recorded at CA3-CA1 synapses (160%, $n=13$ with sc-tPA *versus* 138%, $n=15$ with solvent; $P<0.02$), tc-tPA had no effect (136%, $n=13$) (Figure 8a). Similarly, although long-term depression (LTD) (86%, $n=9$) was selectively reversed into a mild LTP by sc-tPA (107%, $n=10$; $P<0.01$), it was not by tc-tPA

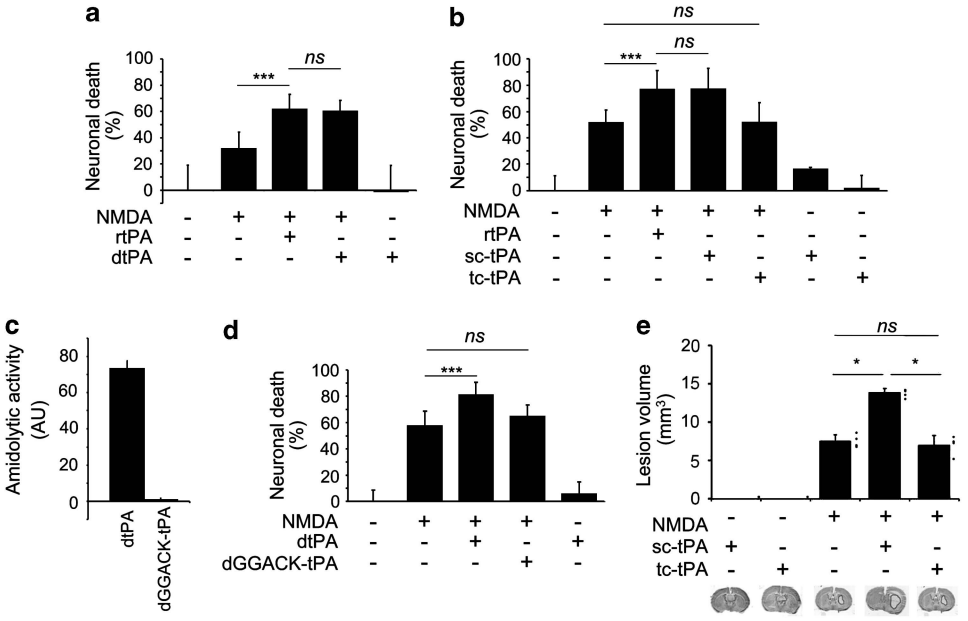

Figure 4 Whereas sc-tPA promotes NMDAR-mediated neurotoxicity through its proteolytic activity, tc-tPA does not. (**a**, **b** and **d**) Neuronal death was assessed by measuring LDH release in the bathing media 24 h after a 1 h exposure of primary cultured cortical neurons (14 DIV) to 50 μM NMDA alone or supplemented with either (**a**) rtPA or dtPA (0.3 μM; $n=12$, four independent experiments), (**b**) rtPA, sc-tPA or tc-tPA at 0.3 μM ($n=16$, four independent experiments), or (**d**) rtPA, dGGACK-tPA at 0.3 μM ($n=12$, three independent experiments). Data are presented as the mean value ± S.D. of neuronal death in percent relative to control. (**c**) Incubation of dtPA with the chloromethylketone dGGACK produced an inactive form of sc-tPA as assayed by fluorogenic assay (dGGACK-tPA). (**e**) NMDA-induced excitotoxic brain lesions measured (thionine staining) 24 h after intrastriatal injections of NMDA (10 mM) either alone or in the presence of either sc-tPA or tc-tPA (45 μM, $n=4$). Data are presented as the mean values ± S.D. of lesion volumes in mm^3 (***$P<0.01$; *$P<0.05$; ns: not significant)

(81%, $n=8$) (Figure 8b). It is noteworthy that neither basal synaptic transmission (Supplementary Figures 3a–d) nor paired-pulse facilitation (Supplementary Figures 3e–g) were affected by sc-tPA (Supplementary Figures 3a, c, e and f) or tc-tPA (Supplementary Figures 3b, d and g). Taken together, these results further identify sc-tPA as the selective activator of postsynaptic NMDARs facilitating synaptic plasticity.

Discussion

tPA is an unusual serine protease produced as an active single-chain enzyme (sc-tPA), sensitive to serpins, rather than a zymogen. In the vascular compartment the low zymogenicity and high intrinsic activity of the sc-tPA requires the formation onto fibrin of a ternary complex with plasminogen to display its full fibrinolytic activity. At the cell surface, plasminogen is rapidly transformed into plasmin which in turn cleaves sc-tPA at Arg275-Ile276, leading to a two-chain enzyme, tc-tPA. Interestingly, in the presence of fibrin both sc-tPA and tc-tPA display the same fibrinolytic activity.[4] Fibrin is therefore an allosteric regulator of tPA fibrinolytic activity.

In the brain parenchyma, tPA interactions extend beyond plasminogen to the NMDAR in the control of functions such as learning processes in the hippocampus (LTP and LTD)[24–26] and dysfunctions such as neurotoxicity.[7,27] Our present data set emphasize the role of tPA molecular form on its interaction with NMDAR in different structures of the central nervous system (CNS). We evidence for the first time a differential function for sc-tPA and tc-tPA in which the exceptional zymogen sc-tPA is the only form of tPA capable to promote NMDAR signaling and subsequent neurotoxicity in cortical and striatal neurons, and LTP in hippocampal neurons. To modulate these functions and dysfunctions, sc-tPA requires its full intrinsic activity, as a proteolytically inactive form of sc-tPA (dGGACK-tPA) failed to promote NMDAR-mediated neurotoxicity. Although, the selectivity of sc-tPA for NMDAR can be observed for concentrations equal or up to 24 nM, tc-tPA was without effect for concentrations up to 300 nM. Even if difficult to measure, we can assume that such concentrations of tPA may be observed in the microenvironment of the synaptic cleft after physiological neuronal depolarization or in pathological conditions such as cerebral ischemia.

Several mechanisms have been proposed to explain the ability of tPA to influence NMDAR signaling,[6,28–30] in accordance with the region of the CNS studied and the experimental paradigm, but in no case a selective effect of sc-tPA has been evoked. The present data point out a mechanism that is dependent on the structure of tPA itself and may therefore be independent of the experimental setting. However, we do not exclude the possibility that other well-described mechanisms may explain the ability of tPA to influence NMDAR signaling: (i) a proteolytic-independent activation leading to an increase in Erk(½)-GSK3 signal transduction pathway[29,31] and (ii) a plasmin-dependent pathway including a proteolytic cleavage of the NMDA receptor[30] leading to an increase in calcium influx.[28] It is nevertheless important to note that experiments in which plasminogen was proposed as the effector of tPA neurotoxicity were performed in the hippocampus and not in the cortex, and that kainate was used in place of a specific NMDAR agonist.[11–13] In a previous

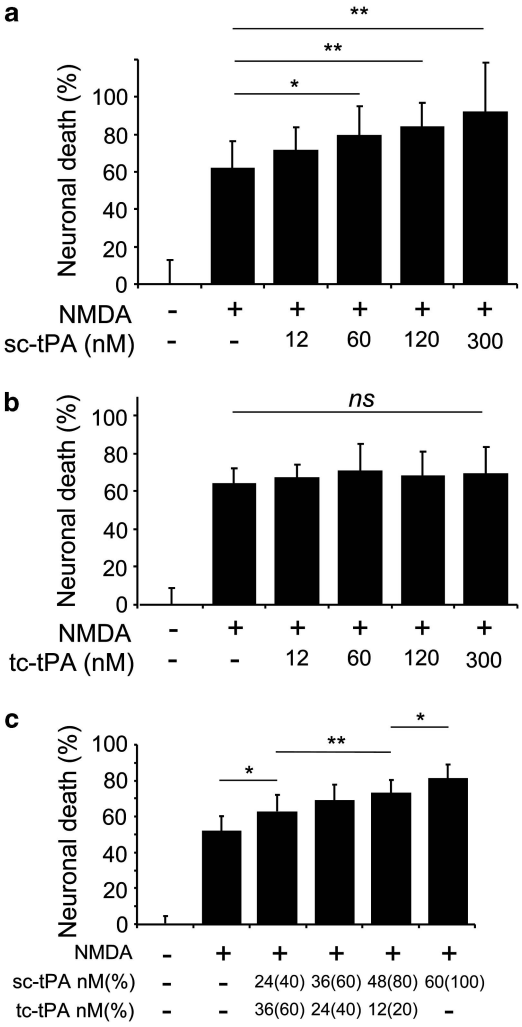

Figure 5 sc-tPA specifically promotes NMDAR-dependent signaling. (**a**–**c**) Neuronal death was assessed by measuring LDH release in the bathing media harvested 24 h after a 1-h exposure of primary cultured cortical neurons (14 DIV) to 50 μM NMDA alone or supplemented with increasing concentrations of either (**a**) sc-tPA or (**b**) tc-tPA (12 nM/60 nM/120 nM/300 nM) ($n=12$, three independent experiments) or (**c**) in the presence of a molar concentration of 60 nM tPA, using differential ratios of sc-tPA and tc-tPA from 40 to 100% ($n=16$, four independent experiments). Data are presented as the mean value ± S.D. of neuronal death in percent relative to control (**$P<0.02$; *$P<0.05$; ns: not significant)

study,[22] we have demonstrated that although tPA promoted NMDAR-mediated neuronal death in cortical neurons, both *in vitro* and *in vivo*, it failed in hippocampic neurons, due to their lack of gluN2D subunit. Moreover, in agreement with our own data, Samson *et al.*[30] reported that tPA potentiated NMDA-induced calcium influx in cortical neurons in a plasmin-independent manner. Here, we performed parallel NMDA-mediated neurotoxicity assays using neuronal cultures maintained in the presence of EACA (ε-amino caproic acid) or aprotinin. As expected no trace of plasminogen or active plasmin was detected in the corresponding cultures. In these conditions, addition of tPA to NMDA led to an increased neurotoxicity, demonstrating an effect of tPA on NMDA-mediated neurotoxicity in cortical neurons independent of the presence of plasminogen or plasmin. *In vivo*, the possibility that plasmin may contribute to the sc-tPA-dependent potentiation of NMDA receptor-mediated neurotoxicity was investigated by intrastriatal coinjections of NMDA and tPA either in wild-type animals in the presence of the specific plasmin inhibitor α2-antiplasmin or in plasminogen-deficient mice. Our data have shown that sc-tPA was pro-neurotoxic in plasminogen-deficient mice, even if the potentiating effect observed was limited. In the wild-type mice, α2-antiplasmin was unable to influence the potentiating effects of sc-tPA. Thus, although our data suggest that sc-tPA promotes NMDA receptor-mediated neurotoxicity independently of plasmin, we cannot exclude that sc-tPA may induce plasminogen-dependent effects in other paradigms. Discrepancies of the amplitude of the potentiating effect of the sc-tPA between wild-type and plasminogen-deficient mice could be explained by a different reactivity of the two strains used (swiss and C57BL/6 J mice, respectively). Other possible explanations are: (i) that because of the lack of plasmin in the plasminogen-deficient mice, the endogenous tPA is mainly single-chain, thus leading to a basal NMDA-induced lesion bigger than in the wild-type animals; (ii) and that in the absence of plasminogen, potential kringle-fixing glycoproteins with exposed lysine residues may considerably reduce the availability of exogenous tPA.

Altogether, our data suggest that abolishing the requirement for proteolysis of tPA could be a mechanism to control its specific functions such as cleavage of NMDAR. Therefore, mechanisms regulating the availability of sc-tPA have key roles in the control of tPA functions and dysfunctions in the nervous system. For example: (i) the neuronal and glial secretions of sc-tPA, (ii) the conversion of sc-tPA into tc-tPA and (iii) the inhibition and the clearance of sc-tPA. For instance, tPA has been shown to be induced as an early gene during seizure kindling and LTP.[32] This transcription of tPA within the brain may be mediated by a specific 5' flanking region that directs appropriate expression in such events.[33] Thus, tPA expression within the brain is strictly controlled and adapted. In addition, two main inhibitors control tPA activity in the brain parenchyma: plasminogen-activator inhibitor 1 (PAI-1) and neuroserpin (NS). Although tPA and NS are usually coexpressed in cerebral tissues, tPA is secreted uncomplexed.[34] Interestingly, in contrast to PAI-1, NS also displays a differential inhibitory action between sc-tPA and tc-tPA. Indeed, Barker-Carlson and collaborators demonstrated that reversible sc-tPA-NS complexes were more stable than those formed with tc-tPA.[35,36]

No loss of sequence takes place during the conversion of sc-tPA into tc-tPA. The selective action of the single-chain form of tPA could be explained by the previous demonstration that tPA interacts with the NMDA receptor through two sites. In this model, both kringle 2 and catalytic domains of tPA were reported to have critical roles for the interaction of tPA with NMDA receptors and subsequent potentiation of NMDA receptors signaling.[37] Thus, we postulate that putative conformational changes occurring following cleavage of the sc-tPA into its two-chain form (R275-I276) may be sufficient to influence accessibility of these tPA's domains to NMDA receptors without any loss in sequence. Other enzymes do not require proteolytic cleavage, and thus loss in sequence, to develop a biological function such as the cysteine proteinase caspase-9, a key enzyme of the apoptosome.[38]

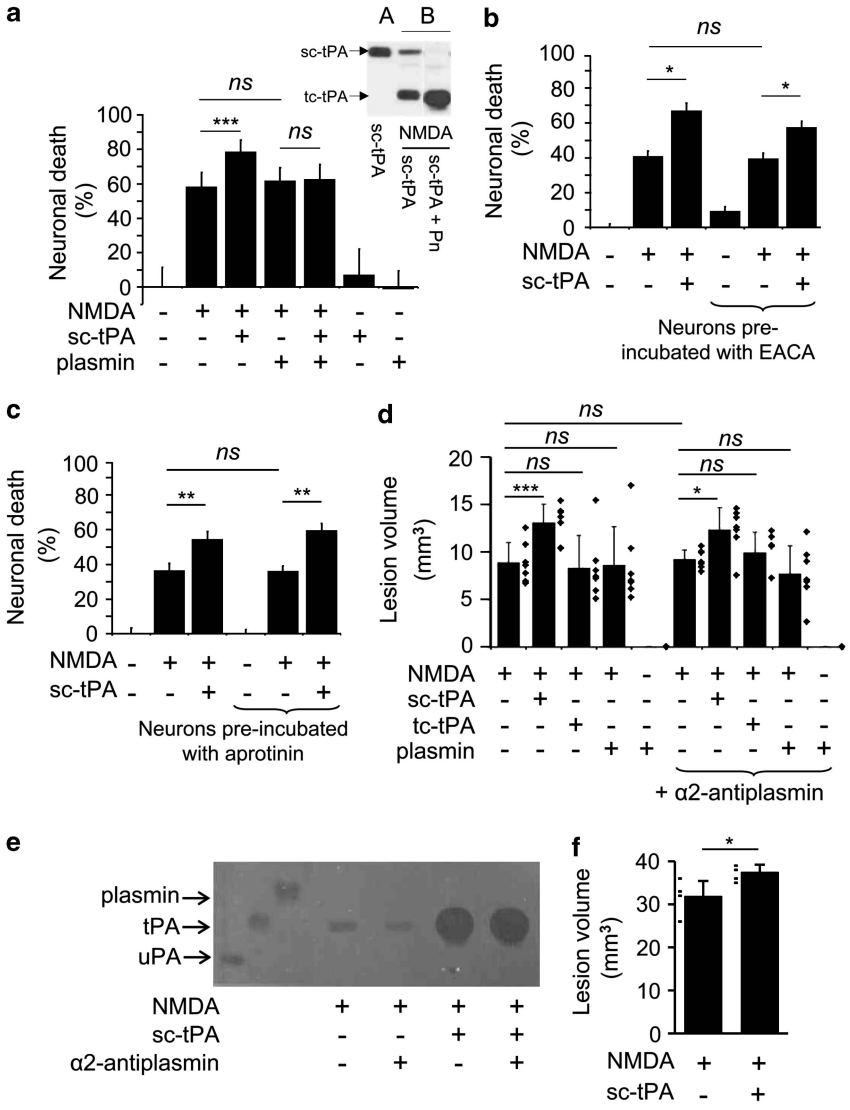

Figure 6 sc-tPA promotes NMDAR-dependent neurotoxicity through a plasmin-independent mechanism. (**a**) LDH released was measured 24 h after a 1-h exposure of primary cultured cortical neurons (14 DIV) to NMDA alone or in the presence of either sc-tPA alone or sc-tPA + plasmin (100 nM; $n=16$, four independent experiments, insert shows conversion of sc-tPA (A) into tc-tPA (B) after an 1 h exposure to neurons). Primary cultures of cortical neurons were plated in the presence or absence of (**b**) EACA (25 mM) or (**c**) aprotinin (1 μM). After 14 DIV, neurons were incubated overnight with 12.5 μM NMDA alone or supplemented with rtPA (0.3 μM, $n=12$, three independent experiments). Data are presented as the mean value ± S.D. of neuronal death in percent relative to control. (**d**) NMDA-induced excitotoxic brain lesions were measured by MRI as described in the methods section, 24 h after intrastriatal injection of NMDA (10 mM) alone or in combination with either sc-tPA (45 μM), tc-tPA (45 μM), or plasmin (150 nM) in the presence or absence of α2-antiplasmin (500 nM, $n=7$). Plasmin (150 nM) and α2-antiplasmin (500 nM) were injected alone as controls. Data are presented as the mean values ± S.D. of lesion volumes in mm^3. (**e**) Zymography assay performed (20 μg of protein extracts) from perfused striatum of swiss mice receiving an intrastriatal injection of either NMDA (10 mM), NMDA + α2-antiplasmin (100 nM), NMDA + sc-tPA (45 μM), NMDA + α2-antiplasmin + sc-tPA (representative of $n=4$ animals per group). Plasmin (200 nM), uPA (0.25 IU/ml) and tPA (0.06 IU/ml) were run in parallel as controls. (**f**) NMDA-induced excitotoxic brain lesion was measured (thionine staining) 24 h after intrastriatal injection of NMDA (10 mM) alone or in combination with sc-tPA (45 μM, $n=5$) in plasminogen null mice. Data are presented as the mean values ± S.D. of lesion volumes in mm^3 (***$P<0.01$; **$P<0.02$; *$P<0.05$; ns: not significant)

To conclude, although in the vascular compartment sc-tPA and tc-tPA display a similar fibrinolytic activity by promoting plasmin formation in the presence of fibrin, sc-tPA is the selective ligand of NMDAR through a proteolytically dependent and plasminogen-independent mechanism (Figure 1). This differential effect of sc-tPA and tc-tPA on NMDAR, in addition to their previously reported differential kinetics of inhibition by NS,[35,36] emphasizes a subtle control of tPA function in the brain. In view of these data, we should reconsider part of the tPA mechanisms reported to influence the brain functions and dysfunctions.

Materials and Methods

Experiments were carried out in accordance with the European Communities Council Directive (86/609/EEC) regarding the care and use of animals for experimental procedures and were approved by the local ethical committee.

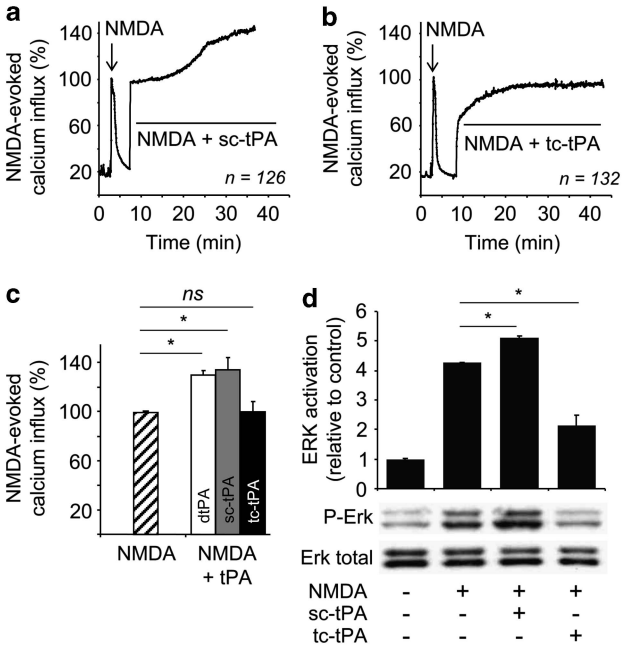

Figure 7 Whereas sc-tPA promotes both NMDA-induced calcium influx and Erk(½) activation, tc-tPA does not. (**a**–**c**) NMDA-induced calcium influx recorded from cultured cortical neurons exposed to NMDA either alone (50 μM) or in the presence of either sc-tPA (**a**: 0.3 μM, $n=126$ cells, three independent experiments) or tc-tPA (**b**: 0.3 μM, $n=132$ cells, three independent experiments). Data are plotted in **c** (dtPA: white bar, sc-tPA: gray bar and tc-tPA: black bar). Data were normalized to NMDA alone (slashed bar). Data are represented as mean value ± S.D. relative to NMDA. (**d**) NMDA-induced Erk(½) activation was evaluated by anti phospho-Erk(½) immunoblotting alone or in the presence of sc-tPA and tc-tPA at a molar concentration of 0.3 μM ($n=3$). Data were normalized to NMDA alone and are represented as mean value ± S.D. of phospho-Erk(½) variation relative to control (*$P<0.05$; ns: not significant)

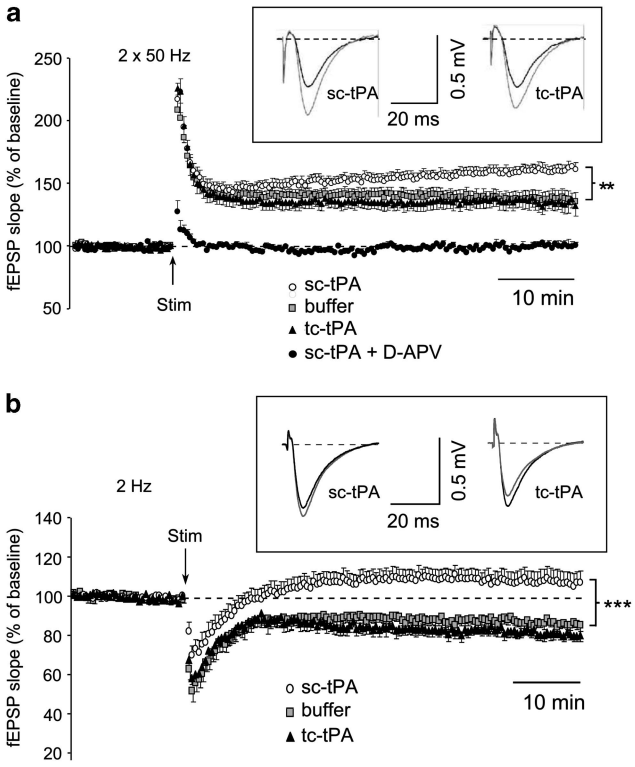

Figure 8 Whereas sc-tPA modulates neuronal synaptic plasticity through NMDAR signaling, tc-tPA does not. (**a**) LTP was recorded in the hippocampal CA1 area in the presence or absence of sc-tPA (100 nM, white dots, $n=13$) and tc-tPA (100 nM, black triangles, $n=13$). APV is used as a control to block NMDA receptors. (**b**) LTD induced alone (gray squares, $n=9$) or in the presence of either sc-tPA (100 nM, white dots, $n=10$) or tc-tPA (100 nM, black triangles, $n=8$). In inserts (**a** and **b**), fEPSPs recorded before and 50 min after stimulation. Statistical analysis was done for this interval using ANOVA repeated measures (**$P<0.02$; ***$P<0.01$)

Chemicals. *N*-methyl-D-aspartate (NMDA) was purchased from Tocris (Bristol, UK). Spectrofluor 444FL was purchased from American Diagnostica (Stamford, CT, USA). Aprotinin, EACA, Dulbecco's modified Eagle's medium (DMEM), poly-D-lysine, cytosine β-D-arabinoside, hygromycin B were from Sigma-Aldrich (L'Isle d'Abeau, France). CNBr-activated Sepharose 4B was from GE Healthcare (Orsay, France), the QuickChange XL site-directed mutagenesis kit from Stratagene (La Jolla, CA, USA). 1,5-dansyl-L-glutamyl-L-glycyl-L-arginine chloromethylketone (dGGACK), plasminogen and α2-antiplasmin were purchased from Calbiochem (Nottingham, UK). Lipofectamine 2000, fetal bovine and horse sera, laminin, FURA-2/AM were from Invitrogen (Cergy Pontoise, France). Plasmin was prepared by activation of plasminogen, purified from fresh frozen human plasma as described,[39] with urokinase-coupled Sepharose 4B. D-2-amino-5-phosphono-valerate (D-APV) was from Ascent Scientific (Weston-super-mare, UK).

Sources of tPA. sc-tPA was purified on immobilized mAb from cultured human melanoma cells (Biopool, Umea, Sweden). A human recombinant tPA purified from Chinese Hamster Ovary cells (Actilyse, 95% single-chain, 5% two-chain tPA) was used either as prepared for medical use (tPA, 2 mg/ml in vehicle containing 34.84 mg/ml arginine, 10.72 mg/ml phosphoric acid, 0.1 mg/ml Tween 80) or dialysed in a buffer containing 0.5 M ammonium bicarbonate to discard arginine (dtPA) using a 10 kDa cut-off membrane. Two-chain tPA (tc-tPA) was prepared by overnight incubation of dtPA with plasmin-coupled Sepharose 4B at 37 °C, followed by a 2 h incubation with immobilized aprotinin to eliminate traces of free plasmin and finally by overnight dialysis in a buffer containing 0.5 M ammonium bicarbonate. Active-site-blocked tPA was obtained by incubating dtPA with a 10-fold molar excess of dGGACK at room temperature for 3 h followed by overnight dialysis in 0.5 M ammonium bicarbonate.

tPA immunoblotting. Immunoblottings were performed using a polyclonal sheep antiserum raised against human tPA (1 : 5000) prepared at the National institute for agronomic research (INRA, Clermont-Theix, France) and a polyclonal rabbit antiserum raised against murine tPA (125 ng/μl), followed by incubation with the appropriate peroxydase-conjugated secondary antibody. Immunoblots were revealed with an enhanced chemoluminescence ECL Plus immunoblotting detection system (Perkin Elmer-NEN, Paris, France).

Clot lysis time. Human plasma was collected and the euglobulin fractions, containing β- and γ-globulins, were separated by dilution of one volume of chilled plasma in 20 volumes of chilled acetic acid 2.9 mM. After incubation at 4 °C for 15 min and centrifugation at 3000 × *g* for 10 min, the euglobulin fraction was precipitated, the supernatant discarded and the precipitate resuspended in HEPES buffer (10 mM HEPES (pH 7.4), 150 mM NaCl). The euglobulin solution (100 μl) was supplemented with 15 mM calcium chloride and 10 IU/ml of the different sources of tPA, and the time to clot lysis was assessed by optical density (405 nm absorbance) at 37 °C. Tests were performed in triplicate. Results were expressed as the time to 50% clot lysis in minutes.

Amidolytic activity assay. The different tPA preparations were incubated in the presence of a fluorogenic substrate (5 μM) (Spectrofluor 444FL). The reaction was carried out at 25 °C in 50 mM Tris (pH 8.0) containing 150 mM NaCl in a total volume of 100 μl. The amidolytic activity of tPA was measured as the change in fluorescence emission at 440 nm (excitation at 360 nm).

SDS-polyacrylamide plasminogen-casein zymography. Zymography assay was performed by addition of plasminogen (4.5 μg/ml) and casein (1%) in 15% SDS-polyacrylamide gels. Electrophoresis was performed at 4 °C. Gels were washed with Triton X-100 (2.5%) and incubated for 2 h at 37 °C. Caseinolytic bands were visualized after Coomassie staining.

Fibrin agarose zymography. Proteins (20 μg) and reference proteins (10 μl of tPA 0.06 IU/ml, uPA 0.25 IU/ml and plasmin 200 nM) were subjected to SDS electrophoresis (8% polyacrylamide gel under non-reducing conditions). SDS was then exchanged with 2.5% Triton X-100. After washing-out excess of Triton X-100 with distilled water, gel were carefully overlaid on a 1% agarose gel containing 1 mg/ml of bovine fibrinogen, 100 nM plasminogen and 0.2 IU/ml of bovine thrombin. Zymograms were allowed to develop at 37 °C during 12 h and photographed at regular intervals using dark-ground illumination. Active proteins in cell lysates were identified by reference to the migration of known markers (uPA, tPA and plasmin).

Neuronal cell culture. Neuronal cultures were prepared from fetal mice (embryonic day 15–16) as previously described.[22] Cortices were dissected and dissociated in DMEM, and plated on 24-well plates previously coated with poly-D-Lysine (0.1 mg/ml) and laminin (0.02 mg/ml). Cells were cultured in DMEM supplemented with 5% fetal bovine serum, 5% horse serum and 2 mM glutamine. Cultures were maintained at 37 °C in a humidified 5% CO_2 atmosphere. Cytosine β-D-arabinoside (10 μM) was added after 3 days *in vitro* (DIV) to inhibit glial proliferation. Various treatments were performed after 14 DIV.

Excitotoxic neuronal death. Excitotoxicity was induced by exposure of cortical neurons to NMDA (50 μM) in serum-free DMEM supplemented with 10 μM of glycine, for 1 h. The different forms of tPA were applied with NMDA when indicated. Neuronal death was quantified 24 h later by measuring the activity of lactate dehydrogenase (LDH) released from damaged cells into the bathing medium by using a cytotoxicity detection kit (Roche Diagnostics, Mannheim, Germany). The LDH level corresponding to the maximal neuronal death was determined in sister cultures exposed to 200 μM NMDA (LDH_{max}). Background LDH levels were determined in sister cultures subjected to control washes (LDH_{min}). Experimental values were measured after subtracting LDH_{min} and then normalized to LDH_{max} – LDH_{min} in order to express the results in percentage of neuronal death relative to control.

p-Erk(½)-dependent NMDAR signaling. Erk(½) activation by phosphorylation was used as an index of NMDAR signaling. NMDARs were activated by exposure of the primary neuronal cultures to the different forms of tPA alone or in the presence of NMDA. After 5 min of treatment, cells were chilled on ice and lysed in buffer containing Tris-NaCl-Triton 1% of protease inhibitor cocktail and 1% of phosphatase inhibitor cocktail. Lysates were clarified by centrifugation at 13 000 $\times$ *g*, for 10 min at 4 °C. Proteins were quantified by Bicinchonic acid protein assay (Pierce, Brebières, France) and immunoblotted using adequate primary antibodies (anti-phosphorylated Erk(½) and anti-Erk(½), at 1/1000 dilution; Cell Signaling, Saint Quentin en Yvelines, France) followed by incubation with the appropriate peroxydase-conjugated secondary antibody. Proteins were then visualized with the ECL Plus immunoblotting detection system. Erk(½) and p-Erk(½) levels were investigated by running separated immunoblots from the same protein extracts.

Excitotoxic lesion. Excitotoxic lesions were performed under isoflurane-induced anesthesia in male swiss mice (25–30 g; CURB, Caen, France). Striatal injections (coordinates: 0.5 mm posterior, + 2.0 mm lateral, − 3.0 mm ventral to the bregma) of 10 nmol NMDA *versus* either NMDA/sc-tPA or NMDA/tc-tPA (10 mM NMDA and 45 μM equivalent amidolytic activity of tPA; total volume of 1 μl) were performed after placing the animals under a stereotaxic frame. In all, 500 nM α2-antiplasmin and 150 nM plasmin were injected when indicated. Injections were made using adapted needles (calibrated at 15 mm/μl; assistant ref 555/5;Hoecht, Sondheim-Rhoen, Germany) and removed 5 min later. After 24 h, brains were collected, frozen in isopentane, cryostat-cutted (20 μm sections), stained with thionine and analyzed (or magnetic resonance imaging (MRI) analyzed).

Plasminogen-deficient (Plg − / −) mice ($n = 5$), backcrossed at least seven generations into C57BL/6J mice, were anesthetized with 4% chloral hydrate (400 mg/kg/IP) before the intrastriatal injection described above. Experiments were approved by the Institutional Animal Care & Use Committee of Emory University (Atlanta, GA, USA).

Magnetic resonance imaging. Experiments were carried out at 24 h following excitotoxic lesions on a Pharmascan 7T (Bruker, Germany). T2-weighted images were acquired using a Multi-Slice Multi-Echo sequences: TE/TR 51.3 ms/1700 ms with 70 $\times$ 70 $\times$ 350 μm^3 spatial resolution. Lesion sizes were quantified on these images using ImageJ (NIH software v1.45r, National Institute of Health, Bethesda, MD, USA).

Calcium imaging. Primary cultures of mice cortical neurons (12–14 DIV) were loaded for 35 min at 37 °C with 10 μM Fura-2/AM resuspended in 0.2% pluronic acid solution and incubated for an additional 15 min at room temperature in HEPES and bicarbonate-buffered saline solution with addition of 10 μM glycine at pH 7.45. Experiments were performed at room temperature with continuous perfusion at 2 ml/min with a peristaltic pump, on the stage of a Nikon Eclipse inverted microscope equipped with a 100-W mercury lamp and oil-immersion Nikon $\times$ 40 objective with 1.4 numerical aperture (Nikon, Tokyo, Japan). Fura-2 (excitation: 340/380 nm, emission: 510 nm) ratio images were acquired every 2 s with a digital camera (Princeton Instruments, Trenton, NJ, USA) using Metafluor 6.3 software (Universal Imaging Corporation, West Chester, PA, USA). Fluorescence ratios (340/380 nM) were converted to intracellular Ca^{2+} concentration using the following formula: $[Ca^{2+}]i = K_d[(R - R_{min})/(R_{max} - R)] F_0/F_s$, where R is the measured ratio of 340/380 fluorescence, R_{min} is the ratio measured in a Ca^{2+}-free solution, R_{max} is the ratio measured in a saturated Ca^{2+} solution, $K_d = 135$ nM (the dissociation constant for Fura-2), and F_0 and F_s are the fluorescence intensities measured, respectively, in a Ca^{2+}-free solution at 380 nM and in a saturated Ca^{2+} solution at 380 nM.

Electrophysiology. The experiments were conducted using adult (3–5 month-old, $n = 21$) mice purchased from Janvier (Le Genest Saint Isle, France). The mice were anesthetized with halothane and decapitated. The hippocampus was quickly removed and placed in ice-cold artificial cerebrospinal fluid (aCSF). The composition of the aCSF was as follows (in mM): NaCl 124, KCl 3.5, $MgSO_4$ 1.5, $CaCl_2$ 2.5, $NaHCO_3$ 26.2, NaH_2PO_4 1.2 and glucose 11. This solution had a pH of 7.35 by bubbling a gas mixture of 95% O_2/5% CO_2. Slices (400 μm thick) were cut and placed into aCSF warmed at 28–30 °C in a holding chamber to facilitate recovery for at least 1 h. A single slice was then transferred to the recording chamber and continuously submerged with the pre-gassed aCSF. Extracellular recordings were obtained at room temperature from the apical dendritic layer of the CA1 area using micropipettes filled with 2 M NaCl. Presynaptic fiber volleys (PFVs) and field excitatory postsynaptic potentials (fEPSPs) were evoked by electrical stimulation of Schaffer collaterals and commissural fibers located in the stratum radiatum. The averaged slope of three PFVs and fEPSPs was measured using Win LTP software.[40] To evaluate the level of receptor activation, the fEPSP/PFV ratio was plotted against stimulus intensity (300, 400 or 500 μA). To investigate LTP of synaptic transmission, a test stimulus was applied every 10 s in control medium and adjusted to get a fEPSP with a baseline slope of 0.1 V/s. The averaged slope of 3 fEPSPs was measured for 15 min before tetanus stimulation, consisting of two high-frequency trains (50 Hz for 1 s at the test intensity), separated by 20 s. Testing with a single pulse was then resumed for 60 min to determine the level of LTP. LTD was induced by the application of low frequency electrical stimulation (LFS), 2 Hz for 10 min. Responses were recorded for 60 min after LFS.

All drugs including the buffer (100 nM), sc-tPA (100 nM), tc-tPA (100 nM) or the NMDAR antagonist D-APV (80 μM) were applied to the aCSF at least 20 min before and during stimulation.

Statistical analysis. All the statistical analyses were performed by the two-tailed Kruskall–Wallis' test, followed by *post-hoc* comparisons, with the two-tailed Mann–Whitney's test or the two-tailed Wilcoxon test when mentioned. Results are expressed as mean ± S.D. relative to control.

Electrophysiological results are expressed as mean ± S.E.M. To take into account the correlations inherent in repeated measures data, *P*-values were calculated using multivariate analyses of variance followed by *post-hoc* unpaired Student *t*-tests. In all cases, differences were considered significant when $P < 0.05$.

Conflict of Interest

The authors declare no conflict of interest.

Acknowledgements. This work was supported by grants from the INSERM (French National Institute for Health and Medical Research) and the Regional Council of Lower Normandy, National Institutes of Health Grants NS-062073 (M Yepes) and HL-095063 (M Yepes), and VA MERIT award BX000474 (M Yepes).

Author Contributions

JP, AFB, RM, TB, AM, JMB, AB, YH, PD, JW and MY performed experiments; HRL provided critical reagents and advice; JP, EAC and DV designed experiments, supervised the project and wrote the manuscript.

1. Angles-Cano E, Balaton A, Le Bonniec B, Genot E, Elion J, Sultan Y. Production of monoclonal antibodies to the high fibrin-affinity, tissue-type plasminogen activator of human plasma. Demonstration of its endothelial origin by immunolocalization. *Blood* 1985; **66**: 913–920.
2. Rijken DC, Hoylaerts M, Collen D. Fibrinolytic properties of one-chain and two-chain human extrinsic (tissue-type) plasminogen activator. *J Biol Chem* 1982; **257**: 2920–2925.
3. Rajapakse S, Ogiwara K, Takano N, Moriyama A, Takahashi T. Biochemical characterization of human kallikrein 8 and its possible involvement in the degradation of extracellular matrix proteins. *FEBS Lett* 2005; **579**: 6879–6884.
4. Thelwell C, Longstaff C. The regulation by fibrinogen and fibrin of tissue plasminogen activator kinetics and inhibition by plasminogen activator inhibitor 1. *J Thromb Haemost* 2007; **5**: 804–811.
5. Baranes D, Lederfein D, Huang YY, Chen M, Bailey CH, Kandel ER. Tissue plasminogen activator contributes to the late phase of LTP and to synaptic growth in the hippocampal mossy fiber pathway. *Neuron* 1998; **21**: 813–825.
6. Nicole O, Docagne F, Ali C, Margaill I, Carmeliet P, MacKenzie ET *et al.* The proteolytic activity of tissue-plasminogen activator enhances NMDA receptor-mediated signaling. *Nat Med* 2001; **7**: 59–64.
7. Yepes M, Roussel BD, Ali C, Vivien D. Tissue-type plasminogen activator in the ischemic brain: more than a thrombolytic. *Trends Neurosci* 2009; **32**: 48–55.
8. Pecorino LT, Darrow AL, Strickland S. *In vitro* analysis of the tissue plasminogen activator promoter reveals a GC box-binding activity present in murine brain but undetectable in kidney and liver. *Mol Cell Biol* 1991; **11**: 3139–3147.
9. Siao C, Tsirka SE. Tissue plasminogen activator mediates microglial activation via its finger domain through annexin II. *J Neurosci* 2002; **22**: 3352–3358.
10. Polavarapu R, Gongora MC, Yi H, Ranganthan S, Lawrence DA, Strickland D *et al.* Tissue-type plasminogen activator-mediated shedding of astrocytic low-density lipoprotein receptor-related protein increases the permeability of the neurovascular unit. *Blood* 2007; **109**: 3270–3278.
11. Tsirka SE, Gualandris A, Amaral DG, Strickland S. Excitotoxin-induced neuronal degeneration and seizure are mediated by tissue plasminogen activator. *Nature* 1995; **377**: 340–344.
12. Tsirka SE, Rogove AD, Strickland S. Neuronal cell death and tPA. *Nature* 1996; **384**: 123–124.
13. Tsirka SE, Rogove AD, Bugge TH, Degen JL, Strickland S. An extracellular proteolytic cascade promotes neuronal degeneration in the mouse hippocampus. *J Neurosci* 1997; **17**: 543–552.
14. Fredriksson L, Li H, Fieber C, Li X, Eriksson U. Tissue plasminogen activator is a potent activator of PDGF-CC. *EMBO J* 2004; **23**: 3793–3802.
15. Lee H, Hwang I, Im H, Koh J, Kim Y. Non-proteolytic neurotrophic effects of tissue plasminogen activator on cultured mouse cerebrocortical neurons. *J Neurochem* 2007; **101**: 1236–1247.
16. Sheehan JJ, Zhou C, Gravanis I, Rogove AD, Wu Y, Bogenhagen DF *et al.* Proteolytic activation of monocyte chemoattractant protein-1 by plasmin underlies excitotoxic neurodegeneration in mice. *J Neurosci* 2007; **27**: 1738–1745.
17. Samson AL, Nevin ST, Medcalf RL. Low molecular weight contaminants in commercial preparations of plasmin and t-PA activate neurons. *J Thromb Haemost* 2008; **6**: 2218–2220.
18. Harston GWJ, Sutherland BA, Kennedy J, Buchan AM. The contribution of L-arginine to the neurotoxicity of recombinant tissue plasminogen activator following cerebral ischemia: a review of rtPA neurotoxicity. *J Cereb Blood Flow Metab* 2010; **30**: 1804–1816.
19. Mannaioni G, Orr AG, Hamill CE, Yuan H, Pedone KH, McCoy KL *et al.* Plasmin potentiates synaptic N-methyl-D-aspartate receptor function in hippocampal neurons through activation of protease-activated receptor-1. *J Biol Chem* 2008; **283**: 20600–20611.
20. Hall SW, Humphries JE, Gonias SL. Inhibition of cell surface receptor-bound plasmin by alpha 2-antiplasmin and alpha 2-macroglobulin. *J Biol Chem* 1991; **266**: 12329–12336.
21. Choi DW. Glutamate neurotoxicity in cortical cell culture is calcium dependent. *Neurosci Lett* 1985; **58**: 293–297.
22. Baron A, Montagne A, Cassé F, Launay S, Maubert E, Ali C *et al.* NR2D-containing NMDA receptors mediate tissue plasminogen activator-promoted neuronal excitotoxicity. *Cell Death Differ* 2010; **17**: 860–871.
23. Pang PT, Teng HK, Zaitsev E, Woo NT, Sakata K, Zhen S *et al.* Cleavage of proBDNF by tPA/plasmin is essential for long-term hippocampal plasticity. *Science* 2004; **306**: 487–491.
24. Calabresi P, Napolitano M, Centonze D, Marfia GA, Gubellini P, Teule MA *et al.* Tissue plasminogen activator controls multiple forms of synaptic plasticity and memory. *Eur J Neurosci* 2000; **12**: 1002–1012.
25. Huang YY, Bach ME, Lipp HP, Zhuo M, Wolfer DP, Hawkins RD *et al.* Mice lacking the gene encoding tissue-type plasminogen activator show a selective interference with late-phase long-term potentiation in both Schaffer collateral and mossy fiber pathways. *Proc Natl Acad Sci USA* 1996; **93**: 8699–8704.
26. Madani R, Hulo S, Toni N, Madani H, Steimer T, Muller D *et al.* Enhanced hippocampal long-term potentiation and learning by increased neuronal expression of tissue-type plasminogen activator in transgenic mice. *EMBO J* 1999; **18**: 3007–3012.
27. Yepes M, Sandkvist M, Wong MK, Coleman TA, Smith E, Cohan SL *et al.* Neuroserpin reduces cerebral infarct volume and protects neurons from ischemia-induced apoptosis. *Blood* 2000; **96**: 569–576.
28. Matys T, Strickland S. Tissue plasminogen activator and NMDA receptor cleavage. *Nat Med* 2003; **9**: 371–372; (author reply 372–373).
29. Medina MG, Ledesma MD, Domínguez JE, Medina M, Zafra D, Alameda F *et al.* Tissue plasminogen activator mediates amyloid-induced neurotoxicity via Erk1/2 activation. *EMBO J* 2005; **24**: 1706–1716.
30. Samson AL, Nevin ST, Croucher D, Niego B, Daniel PB, Weiss TW *et al.* Tissue-type plasminogen activator requires a co-receptor to enhance NMDA receptor function. *J Neurochem* 2008; **107**: 1091–1101.
31. Pawlak R, Melchor JP, Matys T, Skrzypiec AE, Strickland S. Ethanol-withdrawal seizures are controlled by tissue plasminogen activator via modulation of NR2B-containing NMDA receptors. *Proc Natl Acad Sci USA* 2005; **102**: 443–448.
32. Qian Z, Gilbert ME, Colicos MA, Kandel ER, Kuhl D. Tissue-plasminogen activator is induced as an immediate-early gene during seizure, kindling and long-term potentiation. *Nature* 1993; **361**: 453–457.
33. Carroll PM, Tsirka SE, Richards WG, Frohman MA, Strickland S. The mouse tissue plasminogen activator gene 5′ flanking region directs appropriate expression in development and a seizure-enhanced response in the CNS. *Development* 1994; **120**: 3173–3183.
34. Teesalu T, Kulla A, Simisker A, Sirén V, Lawrence DA, Asser T *et al.* Tissue plasminogen activator and neuroserpin are widely expressed in the human central nervous system. *Thromb Haemost* 2004; **92**: 358–368.
35. Barker-Carlson K, Lawrence DA, Schwartz BS. Acyl-enzyme complexes between tissue-type plasminogen activator and neuroserpin are short-lived *in vitro*. *J Biol Chem* 2002; **277**: 46852–46857.
36. Takehara S, Onda M, Zhang J, Nishiyama M, Yang X, Mikami B *et al.* The 2.1-A crystal structure of native neuroserpin reveals unique structural elements that contribute to conformational instability. *J Mol Biol* 2009; **388**: 11–20.
37. Lopez-Atalaya JP, Roussel BD, Levrat D, Parcq J, Nicole O, Hommet Y *et al.* Toward safer thrombolytic agents in stroke: molecular requirements for NMDA receptor-mediated neurotoxicity. *J Cereb Blood Flow Metab* 2008; **28**: 1212–1221.
38. Stennicke HR, Deveraux QL, Humke EW, Reed JC, Dixit VM, Salvesen GS. Caspase-9 can be activated without proteolytic processing. *J Biol Chem* 1999; **274**: 8359–8362.
39. Fleury V, Anglés-Cano E. Characterization of the binding of plasminogen to fibrin surfaces: the role of carboxy-terminal lysines. *Biochemistry* 1991; **30**: 7630–7638.
40. Anderson WW, Collingridge GL. The LTP Program: a data acquisition program for on-line analysis of long-term potentiation and other synaptic events. *J Neurosci Methods* 2001; **108**: 71–83.

Supplementary Information accompanies the paper on Cell Death and Differentiation website (http://www.nature.com/cdd)